Apolipoprotein J and Alzheimer's amyloid β solubility

Etsuro MATSUBARA*, Claudio SOTO, Sam GOVERNALE, Blas FRANGIONE and Jorge GHISO†

Department of Pathology, New York University Medical Center, 550 First Avenue, Room TH 432, New York, NY 10016, U.S.A.

Apolipoprotein J (apoJ) has been found associated with soluble amyloid β (sAβ) in plasma and cerebrospinal fluid in normal individuals and co-deposited with fibrillar Aβ in Alzheimer's cerebrovascular and parenchymal lesions. Although studies *in vitro* and *in vivo* indicate that apoJ is a major carrier protein for sAβ, its role in the fibrillogenesis process is not known. We report herein that apoJ in its native high-density lipoprotein lipidic environment is fully active to interact with Aβ peptides. Furthermore, apoJ prevents aggregation and polymerization of synthetic Aβ *in vitro*. The interaction was stable for at least 14 days at 37 °C in physiologic buffers, and the peptide retrieved after complex dissociation at low pH retained its inherent aggregation properties. In addition, the binding to apoJ protects synthetic Aβ from proteolytic degradation; both Aβ1–42 and Aβ1–40 were more resistant to proteolysis by trypsin and chymotrypsin when complexed to apoJ. The data suggest that the interaction may preclude sAβ aggregation in biological fluids and point to a protecting role of apoJ for complexed Aβ species.

INTRODUCTION

Amyloid β (Aβ), the major constituent of the fibrils deposited into senile plaques and cerebral blood vessels of patients with Alzheimer's disease (AD) and related disorders, is also normally present in body fluids as a soluble component (sAβ) and is secreted by cells in culture (reviewed in [1]). The Aβ peptide extracted from senile plaques of AD patients is mainly 42–44 amino acids long [2–4], whereas the vascular amyloid is primarily shorter at the C-terminus (39–40 amino acids) [5]. Aβ1–40 is also the major form of sAβ, as determined by amino acid sequence analysis [6], although studies employing affinity chromatography, sequence analysis and laser desorption MS identified minor sAβ sequences with heterogeneity and length similar to the Aβ components deposited in senile plaques [7,8]. Therefore it is likely that these forms of sAβ may represent the immediate precursors of the deposited Aβ, linking AD with several types of systemic amyloidosis in which the soluble amyloid precursor circulates as a normal protein [9]. Based on the observations that under certain conditions and concentrations synthetic peptides homologous to sAβ spontaneously polymerize in solution to form amyloid-like fibrils *in vitro* [10–13] and that the presence of cerebrospinal fluid (CSF) prevents fibril formation *in vitro* [14], we hypothesized the existence of plasma and/or CSF factors that maintain sAβ in its soluble form, preventing its aggregation and suppressing its fibril-forming propensity [15]. In support to the first part of the hypothesis, we have identified what appears to be a major plasma and CSF carrier protein for sAβ. The demonstration of a high-affinity interaction ($K_d = 2$ nM) between non-aggregated synthetic Aβ1–40 and apolipoprotein J (apoJ) together with the identification of the complex apoJ–sAβ *in vivo* in CSF and the co-localization of sAβ with apoJ-containing plasma high-density lipoproteins (HDL) suggest that apoJ plays an important role as a carrier molecule for sAβ [15–17]. Albeit with less affinity, other proteins also have the ability to interact and form complexes with synthetic Aβ *in vitro*, among them apoE [18,19], apoA-I [20], apoA-II [20], α1-antichymotrypsin (ACT) [21] and transthyretin (TTR) [22]. Their biological importance as carrier molecules for sAβ is unclear; however, certain apoE isoforms as well as ACT have been shown to modulate fibril formation of synthetic Aβ in experiments *in vitro* [21,23–25]. In addition, apoJ may be related not only to the transport of the soluble peptide in plasma but also to the delivery of sAβ through the blood–brain barrier. Studies *in vivo* performed in guinea pigs have demonstrated the existence of cerebrovascular permeability for Aβ1–40 and human apoJ as well as for the apoJ–Aβ1–40 complex [26,27].

In order to test the hypothesis that the interaction with the carrier molecule maintains the solubility of the peptide, we have designed a simple protocol based on the complex dissociation properties at low pH. Using synthetic Aβ peptides (Aβ1–40 and Aβ1–42) and purified apoJ we were able to demonstrate by reverse-phase HPLC that after several days of incubation at physiologic pH and temperature (conditions that would induce the aggregation of more than 95 % of the native peptide) the complex remained intact and soluble. After being released from the complex, the peptide retained its original structural characteristics and was able to self-aggregate with the same kinetics. Moreover, the complexed forms of the peptides appear to be protected from proteolytic degradation. The data indicate that, under the conditions tested, apoJ appears to prevent the aggregation and degradation of synthetic Aβ peptides *in vitro*.

EXPERIMENTAL

Synthetic peptides, proteins and antibodies

Peptides and proteins

Peptides DAEFRHDSGYEVHHQKLVFFAEDVGSNKGAII-GLMVVGGVV (Aβ1–40) and DAEFRHDSGYEVHHQKLV-

---

FFAEDVGSNKGAIIGLMVVGGVVIA (Aβ1–42), homologous to residues 672–711 and 672–713 of βPP770 respectively, were synthesized at the W. M. Keck Facility at Yale University using N-t-butyloxycarbonyl chemistry. Amino acids were coupled by activated esters and final deprotection/cleavage was performed using hydrogen fluoride. Peptide purification was carried out using a Vydac C18 reverse-phase column and a linear gradient of 0–80 % acetonitrile in 0.05 % trifluoroacetic acid. The final products were lyophilized and characterized by analytical reverse-phase HPLC, amino acid analysis, laser desorption MS and CD. Aβ1–40 had mainly random coil conformation (0 % α-helix, 27.7 % β-sheet, 0.6 % β-turn and 71.7 % random coil) whereas Aβ1–42 had predominantly β-sheet structure (10 % α-helix, 74.5 % β-sheet, 6.4 % β-turn and 9.1 % random coil). A 1 mg/ml stock solution in 50 % acetonitrile of either Aβ1–40 or Aβ1–42 was prepared and frozen at -80 °C until use. Human plasma apoJ was purchased from Quidel (San Diego, CA, U.S.A.); ACT and TTR were obtained from Calbiochem (La Jolla, CA, U.S.A.). Recombinant apoE isoforms 2, 3 and 4 (apoE2, ApoE3 and apoE4) were obtained from PanVera (Madison, WI, U.S.A.). In all cases, protein purity was corroborated by SDS/PAGE and N-terminal sequence analysis.

Antibodies

Polyclonal anti-apoJ 1535 was prepared in 12-week-old New Zealand White rabbits using a synthetic peptide, QLNEQFN-WVSELAN (homologous to positions 134–147 of the apoJ β-chain), coupled to keyhole limpet haemocyanin (Sigma; St Louis, MO, U.S.A.). After an initial injection of 250 μg of antigen dissolved in 0.5 ml of sterile 0.15 M NaCl solution and emulsified with 0.5 ml of monophospholipid A–synthetic trehalose dicorynomycolate (RIBI; Immunochem Research, Hamilton, MO, U.S.A.), rabbits were boosted every 15 days with the same amount of antigen dissolved in 0.15 M NaCl without adjuvant. After 8 weeks, test bleedings were obtained and analysed by ELISA for the presence of specific antibodies. Monoclonal IF12 antibody [anti-(apoJ α-chain)] was a generous gift from Dr. N. H. Choi-Miura [28]; alkaline phosphatase-conjugated goat F(ab')$_2$ anti-mouse IgG was purchased from BioSource (Camarillo, CA, U.S.A.); alkaline phophatase-labelled streptavidin and horseradish peroxidase-labelled goat anti-mouse F(ab')$_2$ were obtained from Amersham (Arlington Heights, IL, U.S.A.); monoclonal 6E10 (anti-Aβ1–17) [29] was purchased from Senetek (Maryland Heights, MO, U.S.A.).

HDL

Human HDL were isolated by preparative gradient ultracentrifugation [16] from fresh human plasma obtained from normal healthy subjects, ages 25–40 years, after a 10–12 h fast. In all cases, centrifugations were performed at 16 °C at 100000 g using a Beckman Ti 50.2 rotor, and densities were adjusted to the necessary values with solid KBr. Briefly, starting plasma was first depleted of very-low- and low-density lipoproteins by ultracentrifugation for 16 h at a density of 1.063 g/ml. Infranatants were re-adjusted to a density of 1.21 g/ml, and HDL were recovered after a 40 h centrifugation, extensively dialysed against 20 mM Tris/HCl/150 mM NaCl/1 mM EDTA, pH 7.2, and stored at 4 °C. HDL were characterized by Tris/Tricine SDS/PAGE (12.5 % gels), immunoblotting with specific antibodies directed against different apolipoproteins and electron microscopy [16]. The protein content of the HDL preparation was measured by the method of Bradford (BioRad; Hercules, CA, U.S.A.), employing BSA as a standard. The concentration of apoJ in HDL was estimated by a double-antibody sandwich ELISA assay [28] using two anti-apoJ antibodies. Briefly, microtitre plates (Immulon 2, Dynatech Lab.; Chantilly, VA, U.S.A.) were precoated with polyclonal 1535 [anti-(apoJ β-chain)] and sequentially incubated with HDL samples followed by monoclonal IF12 antibody [anti-(apoJ α-chain)], which had been conjugated to alkaline phosphatase, as described previously [28]. Colour was developed with p-nitrophenyl phosphate and evaluated at 405 nm on a 7520 Microplate Reader (Cambridge Technology; Watertown, MA, U.S.A.). Purified apoJ of known concentration (estimated by amino acid composition) was used as a standard.

Solid-phase binding studies

The interactions apoJ–Aβ1–40 and apoJ–Aβ1–42 were studied by ELISA, using Aβ1–40, Aβ1–42 and purified apoJ. Polystyrene microtitre plates (Immulon 2) were coated either with Aβ1–40 or Aβ1–42 (400 ng/100 μl per well) in 0.1 M NaHCO$_3$, pH 8.6, for 2 h at 37 °C. Under these conditions, 10 ng of Aβ1–40 and 9.6 ng of Aβ1–42 (representing 2.5 % and 2.4 %, respectively, of the peptide offered) remained bound to the well, as determined by a modification of the Quantigold assay (Diversified Biotech; Boston, MA, U.S.A.). After blocking with 1 % BSA, different concentrations of purified apoJ (0–62.5 nM; 100 μl/well) in 20 mM phosphate/150 mM NaCl at different pH (7.4, 6.0 and 5.0) were added to Aβ1–40- or Aβ1–42-coated wells and incubated for 3 h at 37 °C. Bound apoJ was detected with monoclonal IF12, followed by alkaline phosphatase-conjugated goat F(ab')$_2$ anti-mouse IgG (1:3000). The reaction was developed for 30 min with p-nitrophenyl phosphate in diethanolamine buffer (BioRad), stopped with 0.4 M NaOH, and quantified at 405 nm. Nonspecific binding was determined using BSA-coated wells and/or omitting apoJ in the assay. Binding data were analysed by nonlinear regression with the aid of curve-fitting software (GraphPad Prism Version 1.03, GraphPad Software; San Diego, CA, U.S.A.).

Solid-phase inhibition assays

Competitive inhibition of biotin-labelled apoJ binding to Aβ1–40 and Aβ1–42

A 100 μg portion of apoJ was biotinylated with sulpho-NHS biotin (Pierce; Rockford, IL, U.S.A.) according to the manufacturer's specification; biotin-labelled apoJ was separated from free biotin by chromatography over Sephadex G-10 (Pharmacia; Piscataway, NJ, U.S.A.) equilibrated in 20 mM phosphate/150 mM NaCl, pH 7.2 (PBS). Increasing concentrations (0–1750 nM) of either native unlabelled apoJ or HDL–apoJ were co-incubated with 25 nM of biotin-labelled apoJ in PBS at different pH (7.4, 6.0 and 5.0) in Aβ1–40- or Aβ1–42-coated wells (400 ng/well) for 3 h at 37 °C. Bound biotinylated apoJ was detected with alkaline phophatase-labelled streptavidin (1:1000) and evaluated as described above.

Competitive inhibition of apoJ binding to Aβ1–40 and Aβ1–42

Competitive inhibition assays were performed with apoE2, apoE3, apoE4, ACT and TTR. Solutions (0–2500 nM) of the various competitors were co-incubated with 25 nM of apoJ in Aβ1–40- or Aβ1–42-coated wells (400 ng/well) for 3 h at 37 °C at different pH (7.4, 6.0 and 5.0). Bound apoJ was determined with monoclonal IF12 followed by alkaline phosphatase-conjugated goat F(ab')$_2$ anti-mouse IgG and developed with p-nitrophenyl phosphate in diethanolamine buffer, as described above.

Complex characterization

Non-SDS/PAGE

The apoJ–Aβ1–42 complex was prepared by incubation of 2.2 μmol of apoJ with 2.2 μmol of Aβ1–42 in 0.1 M Tris/HCl, pH 7.4, for 4 h at 37 °C. The complex was separated on native 8 % non-SDS/PAGE [30], transferred to poly(vinylidene difluoride) membranes (Immobilon P, Millipore; Milford, MA, U.S.A.), using 3-cyclohexylamino-1-propanesulphonic acid, pH 11, containing 10 % (v/v) methanol and 0.1 % SDS, stained with Coomassie Brilliant Blue; and the protein bands were excised and sequenced on a 477A protein sequencer (Applied Biosystems; Foster City, CA, U.S.A.), as described previously [17].

Immunoblot analysis

Aggregated Aβ1–42 [Aβ1–42(agg)] was prepared as follows: 50 μg of the synthetic peptide was dissolved in 100 μl of PBS and incubated at 37 °C for different periods of time (0–72 h). Incubation was terminated by the addition of SDS sample buffer and 5 min boiling. For immunoblot detection, apoJ–Aβ1–42 and apoJ–Aβ1–42(agg) complexes were prepared under identical conditions, using 2.2 μmol of apoJ and 2.2 μmol of either fresh or aggregated peptide. After 4 h of incubation at 37 °C, the complexes were separated on Tris/Tricine SDS/PAGE (10 % gels) and electroblotted on to nitrocellulose membrane (BioRad) using the same conditions described above. Membranes were blocked for 1 h with 5 % low-fat dried milk in PBS containing 0.05 % Tween-20 (PBST) and incubated overnight with monoclonal 6E10 (1 : 500), followed by horseradish peroxidase-labelled goat anti-mouse F(ab′)$_2$ (1 : 2000). Immunoblots were observed with an enhanced chemiluminescence (ECL) detection kit and exposed to Hyperfilm ECL (Amersham). The resulting bands were scanned on a PDI densitometer and evaluated with the Quantity One (Ver. 2.4) image analysis software (PDI; Huntington Station, NY, U.S.A.).

Ligand blotting analysis

In a separate set of experiments, the binding of apoJ to native and 72-h-aggregated Aβ1–42 was studied by ligand-blotting analysis. Peptide aliquots (10 μg each) were separated in Tris/Tricine SDS/PAGE (10 % gels) and transferred to nitrocellulose membranes as described above. After blocking for 1 h with 5 % low-fat dried milk in PBST, half of the gel was reacted with monoclonal 6E10 (anti-Aβ) and the other half was incubated for 3 h at 37 °C with 20 μg of apoJ in PBS followed by monoclonal IF12 (anti-apoJ). Bound antibodies were observed with alkaline phosphatase-labelled goat F(ab′)$_2$ anti-mouse IgGs (1 : 3000) followed by 5-bromo-4-chloroindol-3-yl phosphate and Nitroblue Tetrazolium (Kirkegaard and Perry, Gaithersburg, MD, U.S.A.).

Complex purification

The stability of the apoJ–Aβ1–42 complex at different pH was studied by affinity chromatography [15]. Briefly, synthetic Aβ-affinity matrices were allowed to interact in batch with 10 ml of plasma at 37 °C for 3 h. After extensive washes to remove unbound proteins, bound components were eluted with 100 mM phosphate buffers (pH 7.4, 6.5, 6.0, 5.5 and 5.0), 100 mM acetate buffers (pH 4.5, 4.0, 3.5 and 3.0) or acetic acid (pH 2.5). The elution profile was monitored by absorbance at 280 nm, and bound apoJ was identified by SDS/PAGE and N-terminal sequence analysis, as described above.

For purification of the apoJ–Aβ1–42 complex, a modified reverse-phase HPLC was employed, using a Vydac C4 microbore column (214 TP 52, 0.21 cm × 25 cm; The Separations Group, Hesperia, CA, U.S.A.) and a 25 min 3–70 % linear gradient of acetonitrile in water, pH 3.1 (adjusted with trifluoroacetic acid), at a flow rate of 0.2 ml/min. The elution profile was monitored at 214 nm. The peaks obtained from reverse-phase HPLC were separated by electrophoresis and electroblotted on to nitrocellulose to identify the complex apoJ–Aβ1–42 by immunoblot. Membranes were blocked for 1 h with 5 % low-fat dried milk in PBST and incubated overnight with either monoclonal 6E10 or monoclonal IF12 at 1 : 500 dilution, followed by horseradish peroxidase-labelled goat anti-mouse F(ab′)$_2$ (1 : 2000). Immunoblots were observed with an ECL detection kit and exposed to Hyperfilm ECL.

Aggregation assays

Stock solution of Aβ1–42 was prepared in 50 % acetonitrile, and its concentration was determined by amino acid analysis. Portions of this stock (5 μg) were lyophilized, and incubations were started by adding 50 μl of 0.1 M Tris/HCl, pH 7.4, with or without apoJ (5 μg) at 37 °C. The degree of Aβ1–42 aggregation was monitored at different time points (0–14 days) by measuring the peptide that remained in solution after centrifugation at 16000 g for 5 min. The supernatants were analysed by reverse-phase HPLC, using a Vydac C4 microbore column (214 TP 52; 0.21 cm × 25 cm) on a 25 min linear gradient of 3–70 % acetonitrile containing 0.1 % trifluoroacetic acid (pH 2.1; dissociating conditions for the apoJ–Aβ complex). Aβ1–42 was eluted from the column at 58 % acetonitrile (19 min retention time). The area of the peak was used in order to estimate the percentage of the non-sedimentable peptide.

In separate experiments, we tested the aggregation properties of the peptide Aβ1–42 following its dissociation from the complex with apoJ. Aβ1–42 purified by reverse-phase HPLC at pH 2.1 from a 24 h-incubated complex was lyophilized, resuspended in 0.1 M Tris, pH 7.4, at 10 mM concentration and incubated at 37 °C for 24 h and 72 h in the absence of apoJ. Freshly dissolved Aβ1–42 was used as a control. The degree of aggregation was assessed by reverse-phase HPLC after centrifugation as described above.

CD studies

Changes in the secondary structure of Aβ1–42 were evaluated by CD measurements. Spectra in the far UV (260–190 nm) of Aβ1–42 either freshly dissolved or recovered by HPLC from its complex with apoJ were recorded at 24 °C with a Jasco J-720 spectropolarimeter (Jasco Corp.; Tokyo, Japan), using a cell path of 0.1 cm at a peptide concentration of 0.3 mg/ml. Results were expressed in terms of mean residue ellipticity (deg·cm²·dmol^{-1}). CD data were analysed by the Lincomb algorithm [31] to obtain the percentages of the different secondary structure motifs.

RESULTS AND DISCUSSION

We have characterized the apoJ–Aβ1–42 interaction by means of solid-phase ELISA experiments and compared the results with those obtained for the more soluble species Aβ1–40. When increasing concentrations of apoJ were allowed to interact with a constant amount of immobilized peptide at physiologic pH and temperature, a specific, saturable binding was observed. The binding curve fitted to a rectangular hyperbola enabled the calculation of the dissociation constant K_d of 4.6×10^{-9} M (Figure
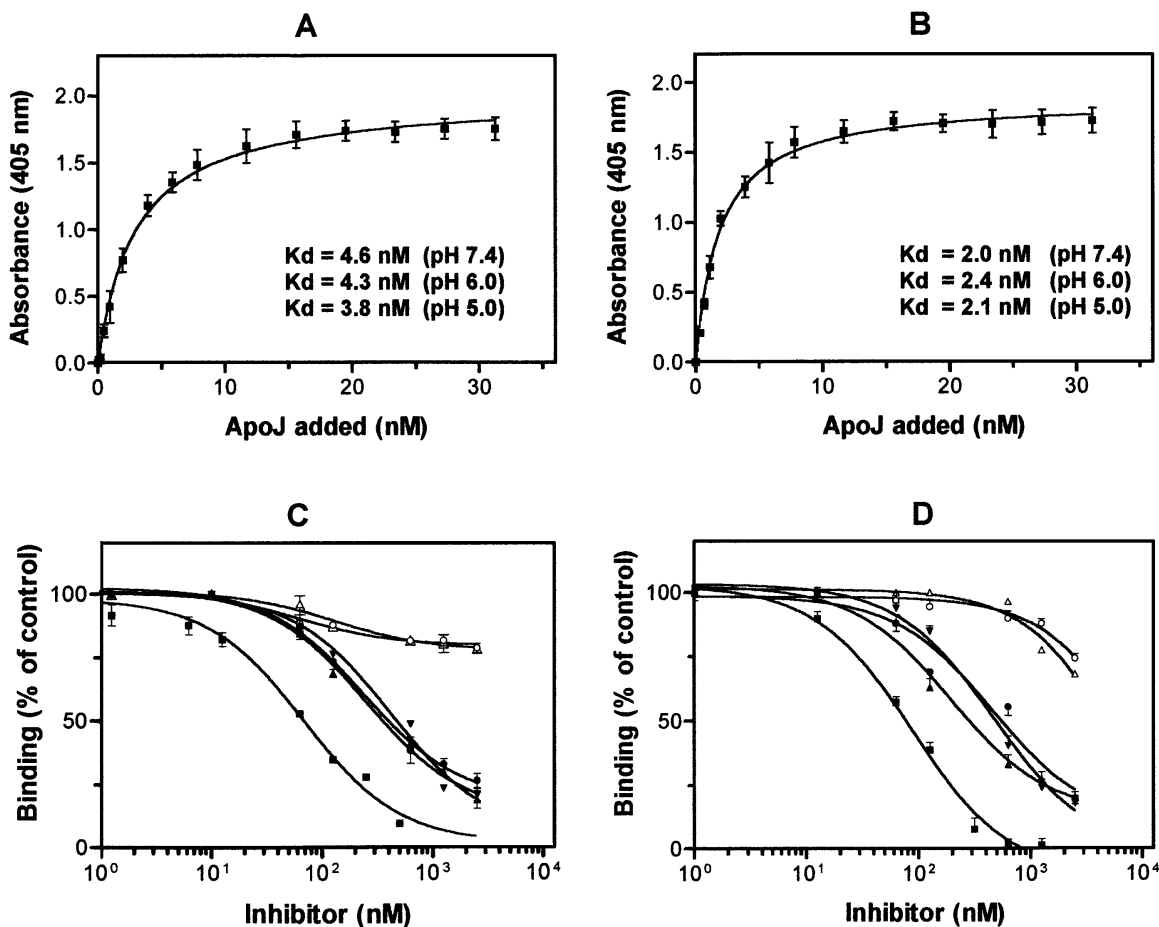
Figure 1   ApoJ–Aβ (Aβ1–42 and Aβ1–40) interaction at variable pH

(**A**, **B**) Saturation curves. Variable concentrations of apoJ (0–62.5 nM) were incubated with either Aβ1–40- (**A**) or Aβ1–42-coated wells (**B**) at variable pH (7.4, 6.0 and 5.0) for 3 h at 37 °C. Bound apoJ was detected with monoclonal IF12 and alkaline phosphatase-labelled anti-mouse as described in the Experimental section. The curves shown were both obtained at pH 7.4. Each point represents the mean (± 2 S.D.) of five independent duplicate experiments. (**C**, **D**) Competitive inhibition of the apoJ–Aβ1–40 (**C**) and apoJ–Aβ1–42 (**D**) complex formation by amyloid-associated proteins. ApoJ (25 nM) was combined with variable concentrations (0–2500 nM) of apoE2 (▲), apoE3 (●), apoE4 (▼), ACT (△) or TTR (○), and co-incubated with either Aβ1–40- (**C**) or Aβ1–42-coated wells (**D**). Bound apoJ was determined as described in the Experimental section. For apoJ self-competition (■), native apoJ (0–1136 nM) was co-incubated with 25 nM biotin-labelled apoJ in either Aβ1–40- or Aβ1–42-coated wells. Bound biotin-labelled apoJ was detected with alkaline phosphatase-labelled streptavidin. Data represent the mean (± 2 S.D.) of three independent duplicate experiments.

1A). The interaction was not affected by pH variations within the range of 5.0–7.4; the corresponding saturation curves (not shown) and the calculated K_d values at pH 6.0 (4.3 nM) and 5.0 (3.8 nM) were not different from the one obtained at pH 7.4. The K_d values for the apoJ–Aβ1–42 interaction were the same order of magnitude as those calculated for apoJ binding to Aβ1–40 (Figure 1B): 2 nM at pH 7.4 [17], 2.4 nM at pH 6.0 and 2.1 nM at pH 5.0. It is interesting to note that conformational changes can be induced in the Aβ peptides by modifying the pH [32]. We have observed the most dramatic changes when Aβ1–40 was used (the amount of β sheet increased from 27.7 % at pH 7.4 to 64.03 % at pH 5.0); Aβ1–42 already contained a high percentage of β sheet at neutral pH (74.5 %), and, therefore, lowering the pH resulted in minimal conformational changes in solution. In our experiments *in vitro* we did not find important differences in the apoJ–Aβ1–40 and Aβ1–42 binding activity when the pH was lowered to 5.0, suggesting either that the interaction is independent of the peptide conformation or that the immobilization to a solid phase induces peptide conformations that are not vulnerable to pH changes.

The specificity of the interaction was tested at physiologic pH by means of inhibition experiments using biotinylated apoJ at a concentration of 25 nM (at which 85–90 % saturation of both Aβ1–40- and Aβ1–42-coated wells was achieved). As indicated in Figure 1(C), the binding of biotin-labelled apoJ to immobilized Aβ1–42 was competitively inhibited by increasing concentrations of native apoJ. The data fitted into a one-site competition curve with a calculated value for half-maximal inhibition (IC_{50}) of 80 ± 18 nM (mean ± 2 S.D.) at pH 7.4, almost identical to the value (77 ± 15 nM) for the inhibition of the interaction between apoJ and Aβ1–40 (Figure 1D; [17]). In addition to apoJ, several other proteins have been implicated in binding interactions with Aβ, among them apoE (isoforms 2, 3 and 4) [18,19], apoAI [20], ACT [21] and TTR [22]. Therefore competitive inhibition experiments of the apoJ–Aβ1–42 complex formation by these proteins were also performed by ELISA. For comparison purposes, competitive inhibition assays for the complex formation between purified apoJ and Aβ1–40 were performed in parallel. Increasing concentrations of each competitor were mixed with constant amounts of apoJ and immediately added to Aβ1–42- or Aβ1–40-
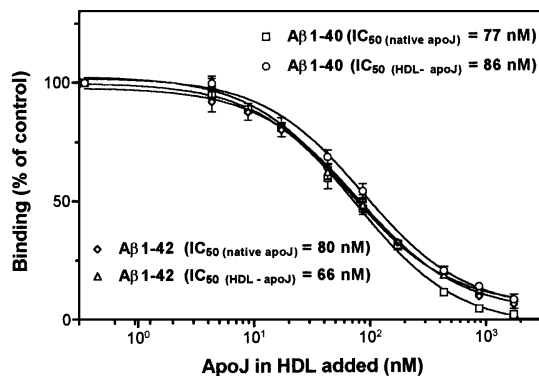
Figure 2   Self-inhibition of the apoJ–Aβ complex formation by apoJ–HDL

Either purified apoJ or HDL particles containing apoJ (0–1750 nM apoJ) were co-incubated with 25 nM biotin-labelled apoJ in either Aβ1–40- or Aβ1–42-coated wells. Bound biotinylated apoJ was evaluated with alkaline phosphatase-labelled streptavidin as described in the Experimental section. Data represent the mean ($\pm$2 S.D.) of three independent duplicate experiments.

coated wells; after 3 h incubation at 37 °C, bound apoJ was detected with anti-apoJ antibody followed by alkaline phosphatase-labelled anti-mouse IgG. Figure 1(C) illustrates the corresponding competition curves in comparison with the apoJ self-inhibition determined by competitive inhibition of biotin-labelled apoJ binding to Aβ1–42 by unlabelled apoJ. None of the proteins tested exhibited higher affinity for Aβ1–42 than apoJ did. The three apoE isoforms showed a similar affinity for Aβ1–42; the calculated IC$_{50}$ values (mean$\pm$2 S.D.) were 245$\pm$46 nM (apoE4), 267$\pm$39 nM (apoE2) and 292$\pm$45 nM (apoE3). The rest of the proteins assayed exhibited very low competitive effects, all in the μmolar range. Although with slightly lower affinity, a similar behaviour has been detected for Aβ1–40 (Figure 1D) [17]; the competition curves distributed themselves into the same two groups, one composed of the apoE isoforms and the other of the rest of the proteins. As in the case of Aβ1–42, none of the proteins tested exhibited better affinity for Aβ1–40 than apoJ did. ApoE2 and apoE4 IC$_{50}$ values were very close (316$\pm$47 and 335$\pm$49 nM respectively), whereas apoE3 was somehow a less avid competitor (508$\pm$44 nM), a behaviour also observed with Aβ1–42. It is important to note that the apoE isoforms used in the competition experiments were recombinant species expressed in Sf9 cells; therefore the effect that lipids may exert in the observed interaction is not known. An important source of variability in these experiments *in vitro* is undoubtedly related to the origin of apoE. The most significant variations have been found in products provided by different manufacturers, but inter-lot variability (in quality and quantity) within the same manufacturer has also been common. In the set of experiments described above, the same provider and the same lot were used. In this context we have found a lower IC$_{50}$ value for apoE4 in competition experiments than our previously published data (335 nM versus 794 nM [17]), differences that might be explained by the different source of apoE4 used in both cases.

In order to test the physiologic relevance of the data, competitive inhibition studies were performed using apoJ in its native HDL environment. HDL particles were purified from normal plasma using the well-established density ultracentrifugation methodology, characterized by gel electrophoresis, immunoblot analysis and electron microscopy [16], and the content of apoJ was estimated by a double-antibody sandwich ELISA assay, using purified apoJ as standard [28]. HDLs were mainly composed of apoAI and apoAII, but also contained apoCII, apoE, apoJ and apoAIV, as previously described [16]. Under the conditions tested, the apoJ concentration in our HDL preparation was estimated as 12.3 ($\pm$1.1) μg per mg of HDL. As indicated in Figure 2, the competition curves virtually superimposed on one another and the corresponding calculated IC$_{50}$ values for purified apoJ and HDL–apoJ were almost identical. The binding of biotin-labelled apoJ to immobilized Aβ1–42 was competitively inhibited by increasing concentrations of apoJ–HDL; the calculated IC$_{50}$ value (66$\pm$19 nM) was within the same range as the one obtained with isolated apoJ (80$\pm$18 nM). When Aβ1–40 was immobilized, the IC$_{50}$ values obtained with apoJ–HDL and isolated apoJ were even closer (86$\pm$20 nM for apoJ-HDL versus 77$\pm$15 nM for isolated apoJ). These results clearly indicate that apoJ, in its lipid environment of the HDL particle, is fully functional to interact with sAβ, supporting the physiological relevance of the interaction.

The decrease of pH from 7.4 to 5.0 did not affect significantly the measured binding affinity between apoJ and either Aβ1–42 or Aβ1–40. However, our previous studies indicated that the complex could be dissociated at very low pH (below 3.0) [15]. In order to determine whether this property might be useful to purify the intact apoJ–Aβ complex from its components, the stability of the complex with the pH was studied in more detail. Synthetic Aβ immobilized on to an affinity matrix was allowed to interact at physiologic pH with normal plasma for 3 h at 37 °C, essentially as described previously [15]. After removing all unbound proteins, elution of bound apoJ was carried out using a discontinuous pH gradient (from 7.4 to 2.5). The pertinent identification of apoJ in the different fractions was carried out by immunoblot analysis and corroborated via N-terminal sequence analysis. As shown in Figure 3(A), apoJ remained bound to the affinity matrix even at pH 3.0 and was completely eluted at pH 2.5, indicating that the complex is stable in a wide pH range and that a narrow threshold below pH 3 would cause its dissociation. Based on this concept, we have designed a simple protocol to isolate the apoJ–Aβ1–42 complex from its components; after incubation of equal concentrations of both apoJ and Aβ1–42 for 4 h at 37 °C (see the Experimental section for details), the mixture was separated on a C4 microbore column using a 25 min 3–70 % linear gradient of acetonitrile in water, adjusted to pH 3.1 with trifuoroacetic acid. A new peak eluting at 62 % acetonitrile (Figure 3B, dashed line) contained the intact apoJ–Aβ1–42 complex, as judged by immunoblot and sequence analyses. An 85 kDa component was recognized by antibodies specific for both Aβ (4G8 and 6E10) and apoJ in immunoblot analysis (results not shown), and N-terminal amino acid sequence analysis after electroblotting retrieved the sequences DQTVSDNELQ, SLMPFSPYEP and DAEFRHDSGY, corresponding to the intact N-terminus of apoJ α-chain, apoJ β-chain and Aβ respectively. When a similar aliquot of the complex was separated in the same column now equilibrated at pH 2.1 (0.05 % trifluoroacetic acid), the complete dissociation of the complex in its components was observed; Aβ1–42 eluted at 58 % acetonitrile whereas apoJ had a longer retention time and was recovered with 65 % acetonitrile (Figure 3B, continuous line). No peaks were detected at 62 % acetonitrile. These results clearly indicate that the apoJ–synthetic Aβ complex can be successfully isolated from its components by a pH-modified reverse-phase methodology.

We have previously reported that apoJ has higher affinity for monomeric Aβ1–40 than for the aggregated peptide; this also applies for Aβ1–42. Complexes were formed by incubation of
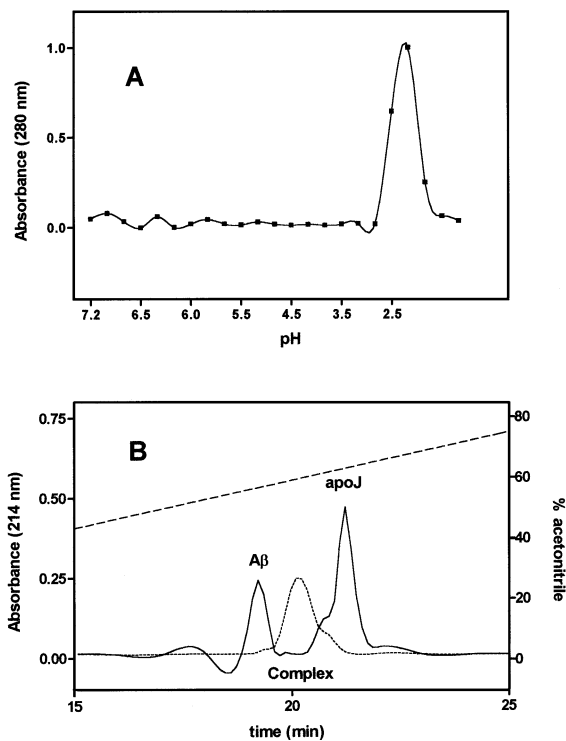
Figure 3   Complex dissociation by pH

(**A**) Affinity chromatography. Synthetic Aβ-affinity matrices were allowed to interact with normal human plasma for 3 h at 37 °C. After washing off the column all the unbound proteins, elution of apoJ was carried out at discontinuous pH (from 7.4 to 2.5) and monitored by absorbance at 280 nm. The presence of apoJ in the different fractions was determined by immunoblot analysis and confirmed by N-terminal sequence analysis. (**B**) Reverse-phase HPLC. apoJ–Aβ1–42 complex was subjected to reverse-phase HPLC under either dissociating (pH 2.1) or non-dissociating (pH 3.1) conditions. Proteins were eluted using a 25 min 3–70 % linear gradient of acetonitrile (– –). Retention times for dissociating conditions: Aβ1–42 = 19 min (58 % acetonitrile); apoJ = 22 min (65 % acetonitrile). Under non-dissociating conditions, the complex was recovered at 62 % acetonitrile (retention time = 20.5 min). Identification was carried out by immunoblot and N-terminal sequence analysis.

Figure 4   Immunodetection of the apoJ-Aβ1–42 complex formed with fresh and/or aggregated peptide

(Left) SDS/PAGE. apoJ–Aβ1–42 and apoJ–Aβ1–42(agg) complexes were prepared in PBS, mixing 2.2 μmol of apoJ and 2.2 μmol of either fresh or 24-h-aggregated Aβ1–42. After incubation, samples were separated by Tris/Tricine SDS/PAGE (10 % gel), immunoblotted with monoclonal 6E10 (anti-Aβ1–17) and observed with horseradish peroxidase-labelled anti-mouse IgG followed by ECL. Lane 1, fresh Aβ1–42 (100 ng); lane 2, 24 h-heat-aggregated Aβ1–42 (100 ng); lane 3, 48 h-heat-aggregated Aβ1–42 (100 ng); lane 4, apoJ–fresh Aβ1–42 complex (100 ng); lane 5, apoJ–24-h-aggregated Aβ1–42 complex (100 ng). M, molecular-mass markers (phosphorylase *b*, 92 kDa; BSA, 67 kDa; ovalbumin, 46 kDa; carbonic anhydrase, 30 kDa; trypsin inhibitor, 20 kDa; lysozyme, 14 kDa; aprotinin, 6 kDa; and insulin β-chain, 3.5 kDa). Arrowhead indicates apoJ–Aβ1–42 complex. (Right) Ligand blot analysis. Freshly prepared (lanes 1 and 3) and 72 h-heat-aggregated Aβ1–42 (lanes 2 and 4) were subjected to electrophoretic separation by Tris/Tricine SDS/PAGE (10 % gel) and transferred to a nitrocellulose membrane. Lanes 1 and 2 were immunoblotted with monoclonal 6E10 followed by alkaline phosphatase-labelled anti-mouse IgG and developed with 5-bromo-4-chloroindol-3-yl phosphate and Nitroblue Tetrazolium. Lanes 3 and 4 were incubated with purified apoJ for 3 h at 37 °C and 16 h at 4 °C. Bound apoJ was detected with monoclonal IF12 [anti-(apoJ α-chain)] and observed as described above. M, molecular weight markers, as in the left panel. Open arrowhead, apoJ–Aβ1–42 complex.

apoJ with fresh and aggregated Aβ1–42 and observed via immunoblot analysis after SDS/PAGE, using monoclonal 6E10 (anti-Aβ1-17), as indicated in Figure 4 (left panel). Scanning densitometry of the fluorograms revealed that apoJ formed 8-fold more 85 kDa complex with the fresh peptide (Figure 4, left panel, lane 4) than with the 24-h-aggregated Aβ1–42 (lane 5). In addition, the polymerization of the peptide was influenced by the presence of apoJ. The aggregation pattern of the freshly prepared Aβ1–42 (Figure 4, left panel, lane 1) remained unmodified following 24 h incubation with apoJ (lane 4), as judged by the similar amount of dimers present and the absence of other higher-molecular-mass polymers. In contrast, the peptide incubated alone for the same period of time under identical conditions showed increased polymerization (Figure 4, left panel, lane 2). In order to test whether apoJ has any effect on the peptide polymerization once the aggregation process has started, apoJ was added to the 24 h-pre-aggregated peptide and incubated for another 24 h. As seen in Figure 4 (left panel), lane 5, the degree of Aβ1–42 aggregation remained unmodified and its pattern resembled the one indicated in lane 2. However, the same peptide incubated in the absence of apoJ (Figure 4, left panel, lane 3) exhibited further polymerization, as indicated by the amount of dimers and higher-molecular-mass oligomers. These results
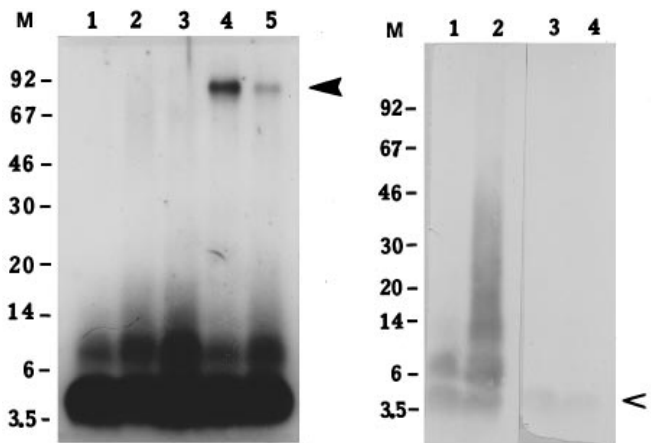
suggest that apoJ might exert a protective effect on sAβ, preventing its oligomerization and aggregation.

To confirm that the binding interaction takes place with the monomeric and not with the polymeric forms of Aβ1–42, we have additionally performed ligand-blotting analysis. Freshly dissolved and 24-h-aggregated Aβ1–42 were fractionated by SDS/PAGE, transferred to a poly(vinylidine difluoride) membrane and allowed to interact with apoJ for 3 h at 37 °C. Bound apoJ was detected with monoclonal anti-apoJ (IF12) followed by alkaline phosphatase-labelled anti-mouse IgG. As indicated in Figure 4 (right panel), apoJ bound only to the monomeric forms of the peptide present in the fresh (lane 3) and 24-h-aggregated (lane 4) preparations. Dimers and higher-molecular-mass components of Aβ1–42 (evidenced by immunoreactivity with monoclonal 6E10; Figure 4, right panel, lanes 1 and 2) did not exhibit visible binding, although the polymeric forms were quantitatively more important than the monomers in the 24-h-aggregated sample. These findings correlate with our previously reported results for the apoJ–Aβ1–40 interaction; inhibition experiments carried out with freshly prepared and 24-h-aggregated Aβ1–40 indicated that the aggregated peptide exhibited 5-fold less relative affinity to form complexes with apoJ (IC$_{50}$ = 315 nM) than with the fresh peptide (IC$_{50}$ = 63 nM) [17].

To test further the influence that apoJ exerts in the aggregation process of the Aβ peptides, we performed a series of HPLC

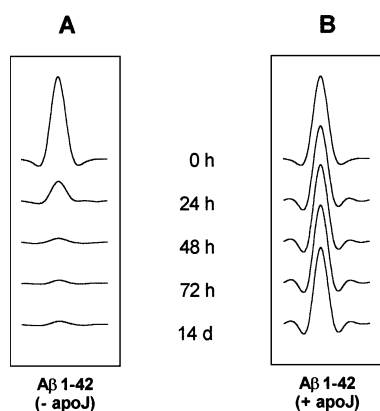**Figure 5   ApoJ prevents the Aβ1–42 self-aggregation**

Aβ1–42 (5 μg aliquots) was incubated at 37 °C in PBS, pH 7.4, for different periods of time in the presence and the absence of apoJ (5 μg). After removing aggregates by centrifugation, the complex was dissociated at pH 2.1 and separated in reverse-phase HPLC as described for Figure 3(B). The amount of the peptide retrieved at 19 min (58% acetonitrile) was evaluated by the area of the eluted peak. (**A**) Aβ1–42 incubated in the absence of apoJ; (**B**) Aβ1–42 incubated in the presence of apoJ.

Figure 6   Aβ1–42 aggregation properties

The aggregation characteristics of freshly dissolved Aβ1–42 (**A**) were compared with those of the peptide retrieved from its complex (Cx) with apoJ after different periods of time (**B**). Evaluation was carried out as in Figure 5. CD spectra for both specimens were recorded (insets) and the respective molar ellipticity plots as well as the calculated secondary structure values are shown.

experiments using the highly aggregable Aβ1–42 , taking advantage of the above-mentioned indication that the intact complex can be purified by reverse-phase HPLC at pH 3.1 and dissociated into its own components at pH 2.0. Identical aliquots of freshly dissolved Aβ1–42 were incubated at 37 °C for different periods of time in the absence or the presence of apoJ at physiologic pH. After incubation, the aggregated components were removed from the soluble forms by centrifugation, and the amount of peptide that remained in solution was determined on reverse-phase HPLC at pH 2.0 (conditions that completely dissociated the complex). The soluble peptide was recovered at its characteristic retention time (19 min, 58 % acetonitrile), and the amount was estimated by the area of the eluted peak. As indicated in Figure 5(A), Aβ1–42 aggregated very fast; 23.5 % of the peptide stayed in solution after a 24 h incubation and only 4 % was left soluble after 48 h, an amount that remained almost constant throughout the rest of the experiment; even after 14 days at 37 °C, 4 % of the peptide was detected in the soluble fraction. When identical aliquots of Aβ1–42 were incubated in the presence of apoJ, the amount of peptide recovered in the HPLC under dissociating conditions was almost the same as the amount retrieved from a freshly prepared complex. For example, after 72 h, 96 % of the peptide remained in solution (Figure 5B) whereas in the absence of apoJ, only 4 % was found in its soluble form (Figure 5A). Moreover, 87 % of the Aβ1–42 incubated with apoJ was still soluble after 14 days at 37 °C. These results indicate that under the conditions tested, the presence of apoJ prevents the aggregation of Aβ1–42 *in vitro*.

In order to test whether Aβ1–42 retained its native properties after being complexed to apoJ, Aβ1–42–apoJ complexes were incubated for 72 h at 37 °C (conditions that would result in 96 % aggregation of the peptide in the absence of apoJ); after centrifugation to remove any aggregates, the soluble complex was dissociated at pH 2.0 and both components, apoJ and Aβ1–42, separated by HPLC. Aβ1–42 recovered from the complex was incubated at 37 °C for different periods of time (up to 72 h), centrifuged to separate newly formed aggregates and evaluated by reverse-phase HPLC in comparison with identical aliquots of freshly prepared Aβ1–42 as a control of non-
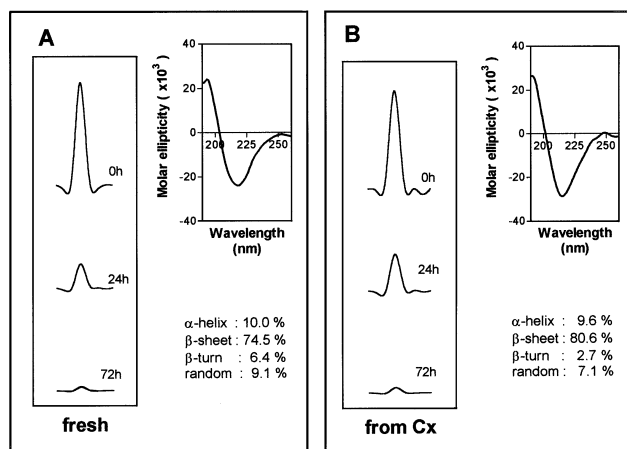
aggregation. As indicated in Figure 6(B), the peptide isolated from the complex aggregated in a similar fashion as the freshly prepared Aβ1–42 (Figure 6A); after 24 h, 27 % of the peptide remained in solution (in comparison with 23.5 % of the fresh Aβ1–42 control) whereas that value dropped to 4.4 % after 72 h. In addition, its CD spectrum was almost identical to that of the fresh Aβ1–42. The secondary structure calculated from the molar ellipticity plots revealed that no substantial conformational changes had been induced in the peptide by the presence of apoJ. Aβ1–42 either recovered from the complex or freshly prepared has predominantly β-sheet structure and possesses full capability to undergo aggregation (Figure 6).

Since the formation of the complex prevented the aggregation of Aβ1–42, we tested whether the interaction also had any influence on the susceptibility of the peptide to proteolytic degradation. Aβ1–40 and Aβ1–42, either native or complexed to apoJ, were subjected to cleavage by trypsin, chymotrypsin and plasmin. Enzymic degradation was evaluated by immunoblot analysis, using monoclonal 6E10 followed by densitometric evaluation of the resulting fluorograms. Time-course experiments indicated that when complexed to apoJ, both Aβ1–40 and Aβ1–42 were more resistant to proteolysis. Chymotrypsin digestion is depicted in Figure 7; after 60 min of incubation at 37 °C, only 20–25 % of both peptides was not degraded by the enzyme whereas 65 % of the apoJ–Aβ1–40 complex and 85 % of the apoJ–Aβ1–42 complex remained undigested. Similar results were obtained with trypsin and plasmin. This protective effect was not seen in control experiments using human apoE or apoAI under the same conditions (results not shown).

The *in vitro* data presented above indicate a high-affinity binding between apoJ and the two main forms of the Aβ peptide, Aβ1–40 predominantly found as the soluble sAβ as well as in cerebrovascular amyloid deposits and Aβ1–42 the main component of the parenchymal senile plaques. The biological importance of the interaction might reside (i) in the maintenance of the sAβ solubility in biological fluids, a concept supported by the existence of the apoJ–sAβ complex *in vivo* in plasma [16] and CSF [15] and (ii) in the blood-to-brain transport of sAβ across the blood–brain barrier. The latter is favoured by the *in vivo*

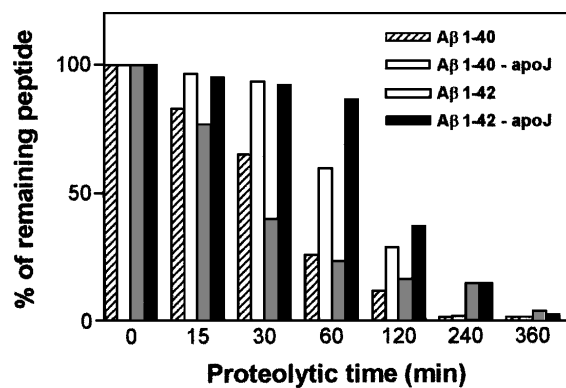**Figure 7   ApoJ protects Aβ peptides from proteolytic degradation**

Aβ1–40 and Aβ1–42 in either the absence or the presence of apoJ were subjected to proteolytic cleavage using chymotrypsin (1:100 w/w) under the conditions described in the Experimental section. After digestion, the remaining peptide was evaluated by immunoblotting with monoclonal 6E10 followed by peroxidase-labelled anti-mouse IgG and ECL. The resulting fluorograms were evaluated by densitometric scanning and image analysis. The percentage of the undigested peptide at each point of the time-course experiment is shown.

experiments performed in guinea pigs that indicate the existence of a specific mechanism at the blood–brain barrier that facilitates the capillary sequestration and transport of Aβ1–40 when complexed to apoJ [26,27], presumably mediated by the receptor for apoJ, gp330 (megalin) [33–35]. Since the apoJ affinities for Aβ1–40 and Aβ1–42 are very close (2.0 and 4.5 nM respectively) it would be expected that apoJ would mediate a similar transport for Aβ1–42 linking AD to several types of systemic amyloidosis where the soluble amyloid precursor is normally found in the circulation [9]. Whether this is only important for the transport mechanism or might sustain a still unknown biological activity of sAβ remains to be determined.

We have previously reported the co-localization of sAβ with apoJ-containing HDL3 and very-HDL in plasma [16]. HDL particles are composed of 54–57 % proteins (primarily apoAI and apoAII) and 43–46 % lipids, mainly esterified cholesterol and phospholipids [36]. Besides apoAI and apoAII, other plasma apolipoproteins are associated to these lipoprotein particles, among them apoE, apoJ, apoC, apoD and apoAIV. ApoJ is mainly bound to apoAI [37,38], although the presence of apoAI is not strictly necessary for apoJ to circulate, as demonstrated by the finding of normal levels of apoJ in patients deficient in apoAI (Tangier disease) [39]. Under physiologic conditions, apoJ in its native HDL lipidic environment is fully active to interact with sAβ; however, the influence that each component of the lipoprotein particle may exert in the interaction between apoJ and sAβ in pathologic situations is not known, particularly those conditions that result in a modification of the relative ratio of the different constituents. The co-localization of apoJ with apolipoproteins with known binding activity for Aβ peptides (apoE isoforms [18,23], apoAI and apoAII [19]) in the same lipoprotein particle suggests a potential competition mechanism for the apoJ–Aβ peptides interaction. In addition, the presence of other plasma proteins that interact with Aβ peptides (ACT [20] and TTR [21]) might further influence the binding activity. Our *in vitro* competitive inhibition studies with many of these isolated Aβ-binding proteins suggest that under physiologic concentrations, the apoJ–Aβ complex formation will take place. Taking into consideration the large carrier concentration excess (1000 × ; low μM versus low nM), it would be expected that all

the sAβ would be complexed to apoJ. However, a more accurate picture of the amount of sAβ that circulates free and/or complexed to apoJ in physiologic as well as in pathologic situations would require the appropriate quantification of both components in different biological fluids.

In summary, the results presented here indicate that (i) a saturable and specific high-affinity binding interaction between apoJ and peptides homologous to the main forms of sAβ (Aβ1–40 and Aβ1–42) can be demonstrated *in vitro*, (ii) the complex formation significantly prevents peptide polymerization and aggregation, and (iii) once the complex is formed, peptides became resistant to proteolytic degradation. The data suggest that the interaction described herein may preclude sAβ aggregation in biological fluids and point to a protecting role of apoJ for complexed Aβ species.

REFERENCES

1 Wisniewski, T., Ghiso, J. and Frangione, B. (1994) Neurobiol. Aging **15**, 143–152
2 Masters, C. L., Simms, G., Weinman, N. A., Multhaup, G., McDonald, B. L. and Beyreuther, K. (1985) Proc. Natl. Acad. Sci. U.S.A. **82**, 4245–4249
3 Selkoe, D. J., Abraham, C. R., Podlisny, M. B. and Duffy, L. K. (1986) J. Neurochem. **146**, 1820–1834
4 Wisniewski, T., Lalowski, M., Levy, E., Marques, M. R. F. and Frangione, B. (1994) Ann. Neurol. **35**, 245–246
5 Prelli, F., Castaño, E. M., Glenner, G. G. and Frangione, B. (1988) J. Neurochem. **51**, 648–651
6 Seubert, P., Vigo-Pelfrey, C., Esch, F., Lee, M., Dovey, H., Davis, D., Sinha, S., Schlossmacher, M., Whaley, J., Swindlehurst, C., McCormack, R., Wolfert, R., Selkoe, D., Lieberburg, I. and Schenk, D. (1992) Nature (London) **359**, 325–327
7 Busciglio, J., Gabuzda, D. H., Matsudaira, P. and Yankner, B. A. (1993) Proc. Natl. Acad. Sci. U.S.A. **90**, 2092–2096
8 Vigo-Pelfrey, C., Lee, D., Keim, P., Lieberburg, I. and Schenk, D. B. (1993) J. Neurochem. **61**, 1965–1968
9 Castaño, E. and Frangione, B. (1991) Brain Pathol. **1**, 263–271
10 Hilbich, C., Kisters-Woike, B., Reed, J., Masters, C. L. and Beyreuther, K. (1991) J. Mol. Biol. **218**, 149–163
11 Burdick, D., Soreghan, B., Kwon, M., Kosmoski, J., Knauer, M., Henschen, A., Yates, J., Cotman, C. and Glabe, C. (1992) J. Biol. Chem. **267**, 546–554
12 Hilbich, C., Kisters-Woike, B., Reed, J., Masters, C. L. and Beyreuther, K. (1994) J. Mol. Biol. **228**, 460–473
13 Snyder, S., Ladror, U., Wade, W., Wang, G., Barrett, L., Matayoshi, E., Huffaker, K., Krafft, G. and Holzman, T. (1994) Biophys. J. **67**, 1216–1228
14 Wisniewski, T., Castaño, E. M., Ghiso, J. and Frangione, B. (1993) Ann. Neurol. **34**, 631–633
15 Ghiso, J., Matsubara, E., Koudinov, A., Choi-Miura, N.-H., Tomita, M., Wisniewski, T. and Frangione, B. (1993) Biochem. J. **293**, 27–30
16 Koudinov, A., Matsubara, E., Frangione, B. and Ghiso, J. (1994) Biochem. Biophys. Res. Commun. **205**, 1164–1171
17 Matsubara, E., Frangione, B. and Ghiso, J. (1995) J. Biol. Chem. **270**, 7563–7567
18 Wisniewski, T. and Frangione, B. (1992) Neurosci. Lett. **135**, 235–238
19 Strittmatter, W. J., Saunders, A. M., Schmechel, D., Pericak-Vance, M., Enghild, J., Salvesen, G. S. and Roses, A. D. (1993) Proc. Natl. Acad. Sci. U.S.A. **90**, 1977–1981
20 Golabek, A., Marques, M. A., Lalowski, M. and Wisniewski, T. (1995) Neurosci. Lett. **191**, 79–82
21 Ma, J., Yee, A., Brewer, H. B., Das, S. and Potter, H. (1994) Nature (London) **372**, 92–94
22 Schwarzman, A. L., Gregori, L., Vitak, M., Lyubski, S., Strittmatter, W. J., Enghilder, J. J., Bhasin, R., Sioverman, J., Weisgraber, K. H., Coyle, P. K., Zagorski, M. G., Talafous, J., Eisenberg, M., Saunders, A. M., Roses, A. D. and Goldgaber, D. (1994) Proc. Natl. Acad. Sci. U.S.A. **91**, 8368–8372
23 Sanan, D. A., Weisgraber, K., Huang, D. Y., Saunders, A., Schmechel, D., Wisniewski, T., Frangione, B., Roses, A. D. and Strittmatter, W. J. (1994) J. Clin. Invest. **94**, 860–869

24 Wisniewski, T., Castaño, E. M., Golabek, A., Vogel, T. and Frangione, B. (1994) Am. J. Pathol. **145**, 1030–1035

25 Castaño, E., Prelli, F., Wisniewski, T., Golabek, A., Kumar, A., Soto, C. and Frangione, B. (1995) Biochem. J. **306**, 599–604

26 Zlokovic, B., Ghiso, J., Mackic, J., McComb, J., Weiss, M. and Frangione, B. (1993) Biochem. Biophys. Res. Commun. **197**, 1034–1040

27 Zlokovic, B., Martel, C. L., Mackic, J. B., Matsubara, E., Wisniewski, T., Frangione, B. and Ghiso, J. (1994) Biochem. Biophys. Res. Commun. **205**, 1431–1437

28 Choi-Miura, N.-H., Tobe, T., Hara, K., Yoshida, H. and Tomita, M. (1990) J. Immunol. Meth. **131**, 159–163

29 Kim, K. S., Miller, D. L., Sapienza, V. J., Chen, C. M. J., Bai, C., Grundke-Iqbal, I., Currie, J. and Wisniewski, H. M. (1988) Neurosci. Res. Commun. **2**, 121–130

30 Bryan, J. K. (1977) Anal. Biochem. **78**, 513–519

31 Perczel, A., Park, K. and Fasman, G. D. (1992) Anal. Biochem. **203**, 83–93

32 Barrow, C. J., Yasuda, A., Kenny, P. T. and Zagorsky, M. G. (1992) J. Mol. Biol. **225**, 1075–1093

33 Kounnas, M. Z., Loukinova, E. B., Stefansson, S., Harmony, J. A., Brewer, B. H., Strickland, D. K. and Argraves, W. S. (1995) J. Biol. Chem. **270**, 13070–13075

34 Saito, A., Pietromonaco, S., Loo, A. K. C. and Farquhar, M. G. (1994) Proc. Natl. Acad. Sci. U.S.A. **91**, 9725–9729

35 Zlokovic, B., Martel, C., Matsubara, E., McComb, G., Zheng, G., McCluskey, R., Frangione, B. and Ghiso, J. (1996) Proc. Natl. Acad. Sci. U.S.A. **93**, 4229–4232

36 Scanu, A. M., Edelstein, C. and Keim, P. (1975) in The Plasma Proteins. Structure, Function, and Genetic Control (Putnam, F. W., ed.), vol. I, pp. 317–391, Academic Press, New York

37 DeSilva, H. V., Stuart, W. D., Duvic, C. R., Wetterau, J. R., Ray, M. J., Ferguson, D. G., Albers, H. W., Smith, W. R. and Harmony, J. A. (1990) J. Biol. Chem. **265**, 13240–13247

38 Jenne, D. E., Lowin, B., Peitsch, M. C., Bottcher, A., Schmitz, G. and Tschopp, J. (1991) J. Biol. Chem. **266**, 11030–11036

39 Choi-Miura, N.-H., Sakamoto, T., Ohtaki, S., Nakamura, H., Ishizawa, S. and Takagi, Y. (1993) Clin. Exp. Immunol. **93**, 242–247